

**Nuclear absorption of low energy pions
and the pion-nucleus optical potential**

J. A. Carr* and H. McManus

Physics Department, Michigan State University, East Lansing, Michigan 48824

K. Stricker-Bauer

Physics Department, University of Maryland, College Park, Maryland 20742

(Received 10 September 1981)

The energy dependence of the optical model parameters for low energy, 0–50 MeV, pions was determined by a compromise fit to pionic atoms, π^+ elastic scattering, and π^{\mp} absorption measurements.

[NUCLEAR REACTIONS Pion-nucleus optical potential, elastic scattering and absorption 0–50 MeV on various targets.]

I. INTRODUCTION

Recent measurements¹ of the nuclear absorption cross sections for low energy pions, together with previous measurements of elastic scattering give, for the first time, the opportunity of making an optical model analysis of low energy pion nucleus

scattering which can be more directly compared with similar analyses of pionic atom data.

II. OPTICAL POTENTIAL

The optical potential used in this analysis is of the form used previously.^{2,3} In standard notation

$$2\omega U = -4\pi \left[p_1 b(r) + p_2 B(r) - \vec{\nabla} \cdot \frac{L(r)}{1 + \frac{4\pi}{3} \lambda L(r)} \vec{\nabla} + \frac{1}{2} (1 - p_1^{-1}) \nabla^2 c(r) + \frac{1}{2} (1 - p_2^{-1}) \nabla^2 C(r) \right] \quad (1)$$

plus the Coulomb term. Here

$$b(r) = \bar{b}_0 \rho(r) - \epsilon_\pi b_1 \delta\rho,$$

$$L(r) = p_1^{-1} c(r) + p_2^{-1} C(r),$$

$$c(r) = c_0 \rho(r) - \epsilon_\pi c_1 \delta\rho,$$

$$B(r) = B_0 \rho^2(r) - \epsilon_\pi B_1 \rho \delta\rho,$$

and

$$C(r) = C_0 \rho^2(r) - \epsilon_\pi C_1 \rho \delta\rho,$$

where ρ is the nucleon density normalized to A , and $\delta\rho$ is the neutron-proton density difference. Capitalized parameters B and C indicate terms arising from true pion absorption, while lower case parameters b and c denote terms arising from single nucleon scattering. Isoscalar and isovector terms are distinguished by the subscripts zero and

one, respectively. The isovector terms B_1 and C_1 are taken to be zero unless otherwise noted. The Lorenz-Lorenz-Ericson-Ericson (LLEE) parameter is denoted by λ . Explicit kinematic factors are

$$p_1 = (1 + \epsilon)/(1 + \epsilon/A),$$

$$p_2 = (1 + \frac{1}{2}\epsilon)/(1 + \frac{1}{2}\epsilon/A),$$

$$\epsilon = \omega/m,$$

and the terms in $\nabla^2 \rho$, $\nabla^2 \rho^2$. It should be emphasized that this form of the potential is taken from theoretical considerations,⁴ and has too many parameters to be determined from fits to experimental data alone. Its advantage is that it separates the reactive content of the optical potential into a part ($\text{Im}B$, $\text{Im}C$) coming from true absorption, which is the entire reactive content for pionic atoms, and a part ($\text{Im}b$, $\text{Im}c$) due to inelas-

tic pion collisions, including charge exchange, which we denote as the quasielastic part. This makes a convenient bridge between pionic atoms and low energy pion nucleus scattering.

In a previous analysis of elastic scattering,³ ReB , ReC were taken from theoretical calculations,⁵ as was the quasielastic reactive part (Imb , Imc). For fixed λ , the two single nucleon parameters \bar{b}_0 , ReC_0 were adjusted to fit elastic scattering or pionic atom level shifts: λ was chosen so that ReC_0 was not too far from its phase shift value. Imb and Imc were calculated from pion-nucleon phase shifts, modified by the effect of the Pauli principle. The reactive parameters due to absorption (ImB , ImC) were taken either from theoretical calculations⁵ (parameter set C) or extrapolated from fits to pionic atom widths (parameter set A). The extrapolation was done assuming the energy dependence given by the calculations of Ref. 5, which indicated a 30% increase in the absorption param-

eters between 0 and 50 MeV. Parameter set C fitted elastic π^+ scattering at 50 MeV, but gave much too small pionic atom widths. Parameter set A gave poor fits to elastic scattering. This is illustrated in Fig. 1, which shows a collection of π^+ elastic scattering experimental results at 30 (Ref. 6), 40 (Ref. 7), and 50 (Ref. 6) MeV, compared with calculations using parameter set A (dashed lines) and parameter set C (solid lines). Parameter values for 50 MeV are given in Ref. 3. Parameter set C , with absorption parameters 65–70% of pionic atom values, clearly gives a better fit to elastic scattering at 50 MeV. Thus the empirical evidence from elastic scattering suggested a decrease in the absorption parameters in the region 0–50 MeV, rather than the increase suggested by simple calculations.⁵ However, elastic scattering is only sensitive to the total reactive content of the optical potential, which includes the quasielastic part.

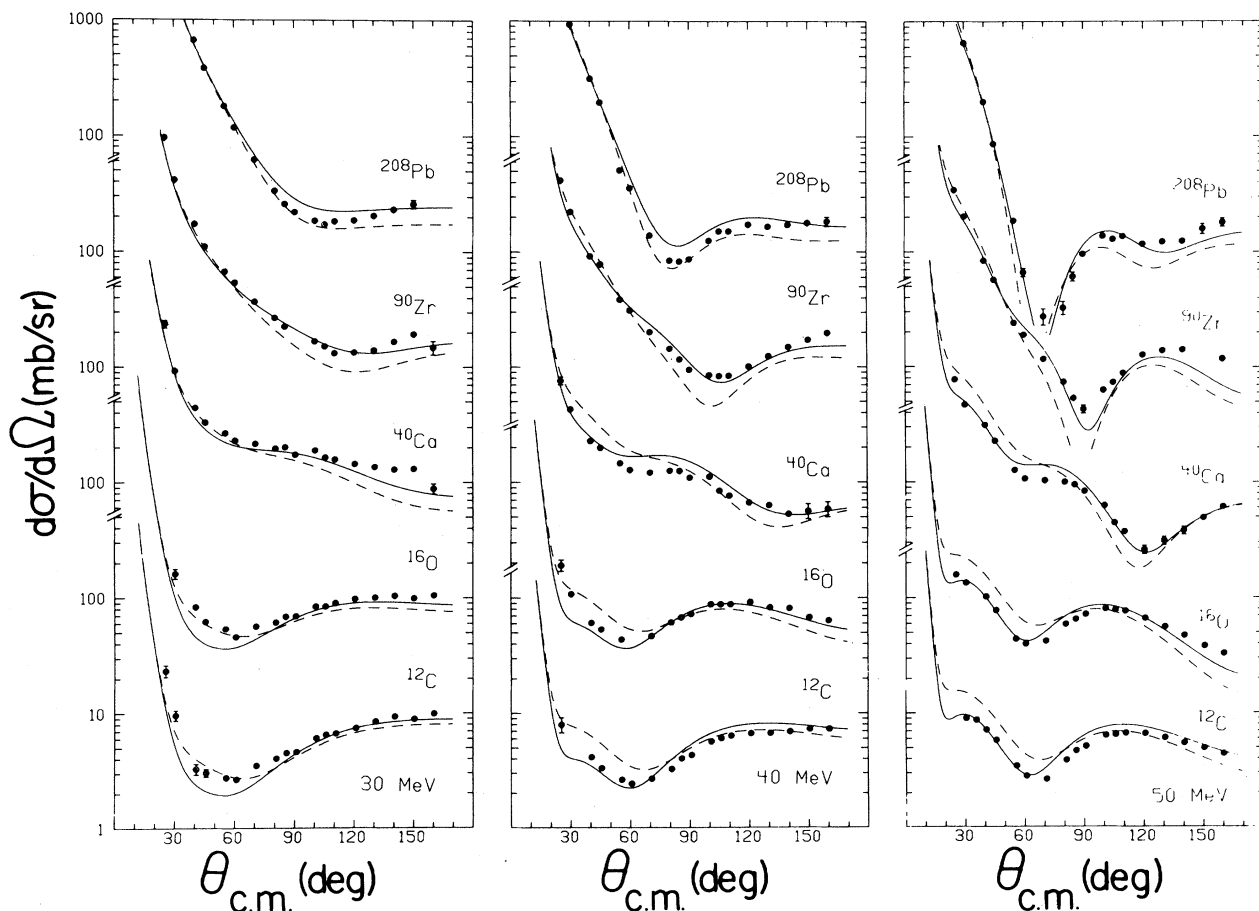


FIG. 1. Elastic π^+ scattering calculations with sets C (solid line) and A (dashed line) defined in Ref. 3. The data are from Refs. 6 and 7.

III. ABSORPTION

The absorption measurements of Ref. 1 now make it possible to independently test the absorption content of these parameter sets. The absorption cross section is calculated from the relation

$$\sigma_{\text{abs}} = \frac{2\pi}{k} \langle \chi | \text{Im}U_{\text{abs}} | \chi \rangle, \quad (2)$$

where χ indicates distorted waves in the complete optical potential and

$$\text{Im}U_{\text{abs}} = -4\pi p_1 \text{Im}B(r) + 4\pi p_2^{-1} \text{Im} \vec{\nabla} \cdot C(r) f(r) \vec{\nabla},$$

where

$$f(r) = \left\{ \left[1 + \frac{4\pi\lambda}{3} \text{Re}L(r) \right]^2 + \left[\frac{4\pi\lambda}{3} \text{Im}L(r) \right]^2 \right\}^{-1}.$$

The justification for the use of relation (2) to calculate a partial cross section is given in Ref. 2. Let us point out that it is always possible to make such an analysis. The reactive part of the optical potential gives the reaction cross section σ_R which is the sum of the partial cross sections σ_{qe} , for inelastic scattering, and σ_a for pion absorption,

$$\sigma_R = \sigma_{qe} + \sigma_a. \quad (3)$$

The reactive part of the optical potential can always be divided in a corresponding way, into the separate contribution of the two channels. The only question that arises is in the interpretation of the resulting parameters, and their connection to microscopic calculations.

The calculated cross sections are compared with the experimental results of Ref. 1 in Fig. 2. Here the open circles are for π^- absorption and the closed circles are measurements of π^+ absorption. The results for parameter set C are given by solid lines (π^+) or dashed lines (π^-). Calculations with parameter set A (extrapolated from pionic atom analysis) are given by the dashed-dotted lines (π^+). The two parameter sets straddle the experimental results.

To get a fix on the absorption parameters and their variation with energy, we took parameter set A, and varied $\text{Im}B$, $\text{Im}C$ in Eq. (2) to fit the measured absorption cross section for each element at each energy, keeping the other parameters constant. As it is only possible to determine one num-

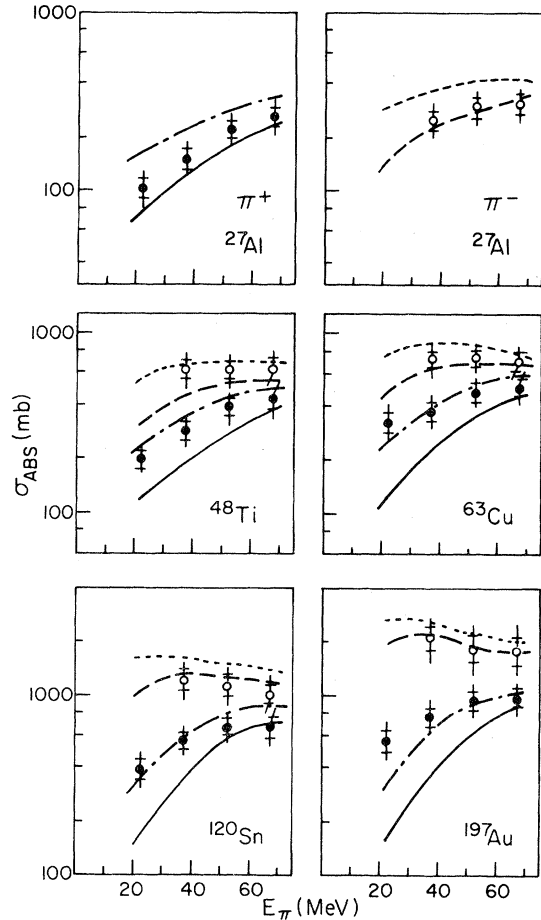


FIG. 2. Absorption calculations with sets C (solid line for π^+ , long dash for π^-) and A (dashed-dotted line for π^+ , short dashes for π^-) defined in Ref. 3. The data are from Ref. 1, with solid circles for π^+ and open circles for π^- . The error bars include the stated 20% normalization uncertainty, with the cross bars indicating the size of purely statistical uncertainties.

ber this way, we kept the ratio $\text{Im}B/\text{Im}C$ fixed at its pionic atom value. This seemed reasonable as there is no reason to expect any rapid energy variation in this energy range.

Figure 3 shows the results of this analysis on the absorption of 23 MeV π^+ , 37 MeV π^\pm , and 52 MeV π^\pm on a variety of elements, where π^+ are solid markers and π^- are open markers. Also plotted at zero energy are the values³ obtained from pionic atoms, an average over light and medium weight nuclei. The plots for $\text{Im}B$ are necessarily identical to those for $\text{Im}C$ from the convention used in fitting. The dotted horizontal curve is simply the pionic atom value put in to aid the eye. The solid curves are the theoretical calculations of Riska and collaborators⁵ (parameter set C). The

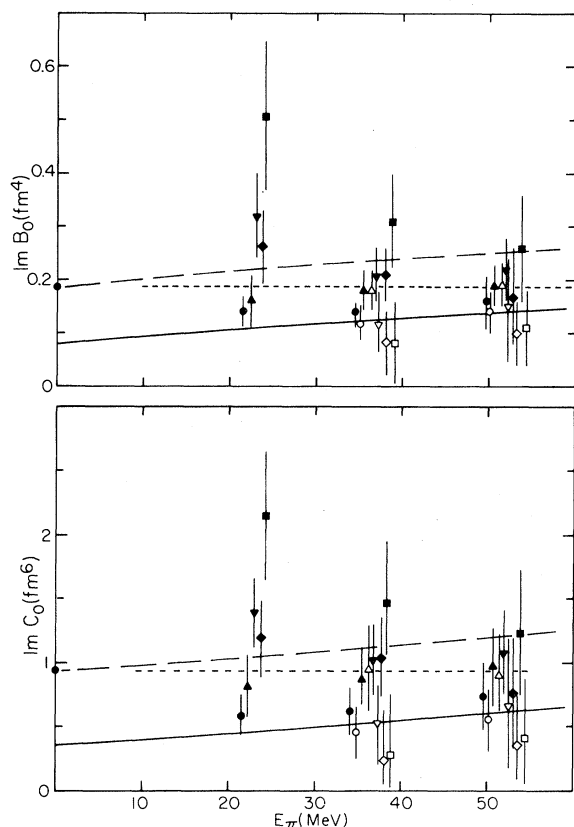


FIG. 3. Values of the absorption parameters required to fit the data of Ref. 1, using the method described in the text. The point at zero energy is the pionic atom (π^-) value determined in Ref. 3. The symbols used are circles for ^{27}Al , triangles for ^{48}Ti , inverted triangles for ^{63}Cu , diamonds for ^{120}Sn , and squares for ^{197}Au . Solid markers are for π^+ , open markers for π^- . The symbols have been displaced horizontally about the experimental energies of 23, 37, and 52 MeV in order of increasing A . The values for set C (solid) and set A (dashed), as well as a horizontal short dashed line at the pionic atom value, are included to help set the scale.

TABLE I. Values of the average p -wave absorption parameters, $\text{Im}C$ (fm^6), required to fit the data of Ref. 1, using the method described in the text. $\text{Im}C_0$ is the isoscalar and $\text{Im}C_1$ the isovector component.

Energy (MeV)	Projectile	$\text{Im}C_0$	$\text{Im}C_1$
0(π -atom)	π^-	0.93	
23	π^+	0.90 ± 0.1	
37	π^\pm	0.73 ± 0.1	2.3 ± 0.9
52	π^\pm	0.78 ± 0.1	1.6 ± 1.1

dashed curves are the same with an additive renormalization to fit the pionic atom data points (parameter set A). The symbols for ^{27}Al , ^{48}Ti , ^{63}Cu , ^{120}Sn , and ^{197}Au have been displaced horizontally about the correct energy in order to maintain readability. The error bars correspond to the statistical errors in the data plus an allowance for a 20% systematic error.

Two points are immediately obvious from Fig. 3. First, the values of the absorption parameters averaged over π^+ and π^- stay quite close to the pionic atom values, as shown by the dotted horizontal line. Second, the π^+ parameters are consistently larger than the π^- parameters for high Z nuclei, indicating a possible isovector absorption component, $\text{Im}B_1$, $\text{Im}C_1$. However, the spread in the mean values for the average of π^+ and π^- parameters is almost as large as the individual π^+ , π^- differences. Ignoring the systematic errors, we obtain the results in Table I. This points to a decrease in the isoscalar absorptive parameters as a function of energy.

IV. ELASTIC SCATTERING

We now return to elastic scattering using the new information on the absorptive parameters. As there is considerable scatter in these values, we use as a bench mark pionic atom values, which are close to the mean, and in the absence of π^- scattering data, ignore a possible isovector component. The other parameters are those of set A . The results are shown in Fig. 4, which compares measured⁶ 50 MeV π^+ scattering from ^{16}O , ^{40}Ca , and ^{208}Pb with the calculations. The dashed curves correspond to pionic atom absorption parameters and thus to a fit on the average to the absorption measurements. The other curves show the effect of varying the absorption parameters, the solid curve corresponding to 60%, the dotted curves to 140%, of pionic atom values. The elastic scattering data shows a definite preference for absorption parameters about 60% of pionic atom values, in agreement with the calculations presented in Fig. 1.

To make a more precise comparison, we took the absorption parameter $\text{Im}C_0$ from Table I, i.e., 83% of its pionic atom value, with a corresponding value for $\text{Im}B_0$, and varied the single nucleon parameters $\text{Re}\bar{b}_0$, $\text{Re}c_0$ to get a best fit to the elastic scattering data of Refs. 6 and 7. The values obtained were -0.063 fm and 0.70 fm³ (parameter set D). The other parameters were left as in

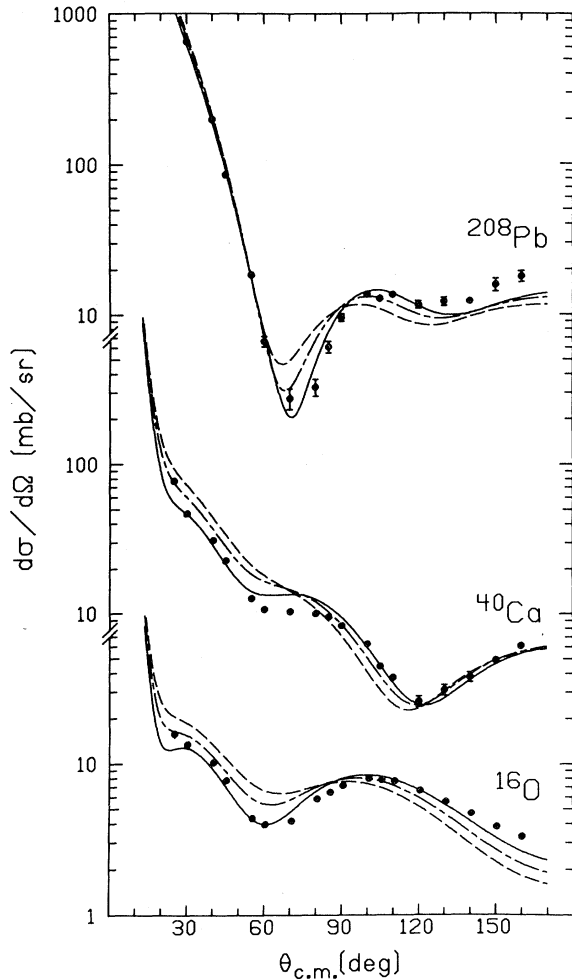


FIG. 4. Elastic scattering of 50 MeV π^+ compared to some of the data from Ref. 6. The curves show the best fit results with varying amounts of absorption in the reactive part of the optical potential. The values used are 60% (solid curve, also set *E*), 100% (dashed-dotted curve), and 140% (dashed curve) of the pionic atom parameters.

parameter set *A*. To check that the results were not sensitive to the particular choice of the LLEE parameter λ , we repeated the calculation for several other values of λ , making corresponding adjustments to $\text{Im}C_0$ to keep the absorption cross section constant. This then represented the best compromise between fitting the elastic and the measured absorption cross sections, without altering the quasielastic parameters $\text{Im}b$, $\text{Im}c$. However, the elastic fit was unsatisfactory ($\chi^2/\text{point}=2.6$). Repeating the calculations for ^{208}Pb using an isovector component $\text{Im}C_1 = \text{Im}C_0$

made little difference. We could get a good fit to the elastic scattering only by reducing the reactive part of the optical potential, either by reducing $\text{Im}C_0$ by 60% keeping $\text{Im}B_0/\text{Im}C_0$ fixed at the pionic atom value (parameter sets *E*), or by reducing the quasielastic reactive parameters $\text{Im}b$, $\text{Im}c$ by 60%, keeping the ratio $\text{Im}b/\text{Im}c$ fixed and the absorption at 83% of pionic atoms (parameter sets *F*). The partial cross sections obtained (for $\lambda=1.4$) together with the fit to elastic scattering expressed as χ^2/point are given in Table II.

The sets *E* and *F* which give best fits to the elastic scattering give nearly the same reaction cross sections. Set *D*, with fixed reactive parameters which do not give as good a fit to elastic scattering, leads to larger reaction cross sections. The above results are typical and hold for a wide range of the parameter λ . We infer that they are not too dependent on the precise form of the optical potential used, provided it is a local potential of the Kisslinger type. The elastic scattering measures the reactive content of the optical potential as expressed in the reaction cross section.

V. QUASIELASTIC SCATTERING

A choice between these sets depends on what evidence there is for the magnitude of quasielastic cross sections. The theoretical estimates used in parameter sets *D* and *E* come from phase shifts corrected for the Pauli principle using the Fermi gas model. A check on these estimates was performed for 50 MeV π^+ scattering from ^{40}Ca , using a DWIA calculation summing up the contribution from collective modes. This gave $\sigma(\pi, \pi') = 64$ mb. Adding charge exchange gives an estimate $\sigma_{qe} \sim 85$ mb, in rough agreement with the estimates in Table II. Experimental evidence is scanty. Bowles *et al.*⁹ have measured the charge exchange cross section for 50 MeV π^+ on ^{16}O as 21 ± 3 mb, from which they infer a quasielastic cross section of ~ 68 mb. Also, Amann *et al.*¹⁰ have measured $\sigma(\pi, \pi')$ for 67 MeV π^+ on ^{12}C as 73 ± 25 mb, which extrapolates to 49 ± 17 mb for 50 MeV π^+ on ^{12}C , or $\sigma_{qe} \sim 67 \pm 20$ mb, allowing for charge exchange. These are estimates only, but clearly indicate a quasielastic cross section of 50–60 mb for 50 MeV π^+ on ^{16}O , rather than the 30 mb as given by parameter set *F*. We therefore adopt set *E* as the most reasonable compromise at the moment, pending further information.

TABLE II. Partial cross sections in mb for 50 MeV π^+ scattering, corresponding to the various parameter sets described in the text and the average χ^2/point for the fit to elastic scattering.

Parameter set	χ^2/pt	^{16}O			^{40}Ca			^{208}Pb		
		σ_R	σ_a	σ_{qe}	σ_R	σ_a	σ_{qe}	σ_R	σ_a	σ_{qe}
<i>D</i>	2.6	173	124	49	364	260	104	966	721	245
<i>E</i>	1.8	148	95	53	327	211	116	901	615	286
<i>F</i>	2.1	158	129	30	342	278	64	935	783	151
<i>K</i> ₁	2.2	164			363			861		
<i>K</i> ₂	1.6	191			401			911		

VI. RESULTS

Table III gives the calculated absorption and reaction cross sections for this parameter set, compared with the measured absorption cross sections. The predicted absorption cross sections from set *E* are about 20% too low for π^+ , and about 10% too low for π^- . However, the measured absorption cross sections for π^+ are uncomfortably close to the reaction cross sections σ_R (calc) deduced from the fit to elastic scattering. Also, if the absorptive parameters are increased at the expense of the reactive part of the quasielastic parameters, as in going from set *E* to set *F*, the π^- absorption cross sections increase much more rapidly than the π^+ absorption cross sections, and trying to improve

agreement with the π^+ leads to poorer agreement with the π^- cross sections. As the normalization uncertainties in the absorption measurements are stated to be $\sim 20\%$, parameter set *E* and the results of Table III would seem to be an acceptable compromise. These give quasielastic cross sections about half the absorption cross sections at 50 MeV, for both π^+ and π^- . The measured absorption cross sections quoted in Table III are quite closely proportional to $A^{2/3}$ for both π^+ and π^- . The calculated values have approximately the same dependence for π^+ , but vary somewhat more rapidly for π^- .

Table IV gives parameter set *E* at 50 MeV, the corresponding potential for pionic atoms and the potential interpolated at 25 MeV. The values of

TABLE III. Reaction and absorption cross sections at 50 MeV calculated from parameter set *E* together with the measured absorption cross sections from Ref. 1, at 52 MeV. The ratio of calculation to experiment gives the size of the systematic differences that can be seen in Fig. 5.

		σ_R (calc)	σ_a (calc)	σ_a (expt)	σ_a (calc)/ σ_a (exp)
π^+	^{27}Al	263	168	220 ± 15	0.76
	^{48}Ti	427	278	395 ± 25	0.70
	^{63}Cu	509	329	490 ± 25	0.67
	^{120}Sn	783	520	664 ± 25	0.78
	^{197}Au	938	627	945 ± 60	0.66
π^-	^{27}Al	414	271	307 ± 20	0.88
	^{48}Ti	757	503	637 ± 20	0.79
	^{63}Cu	1001	664	758 ± 20	0.88
	^{120}Sn	1797	1204	1130 ± 30	1.06
	^{197}Au	2769	1871	1781 ± 40	1.05

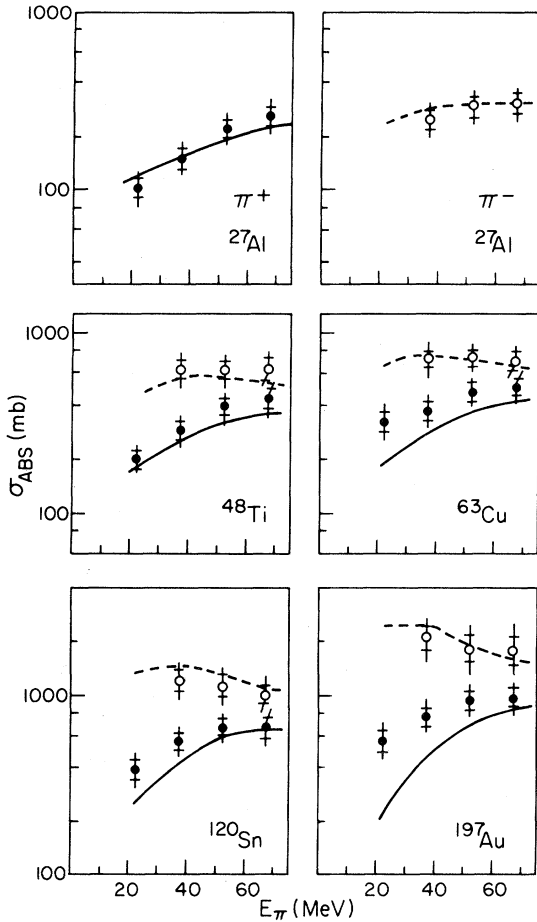


FIG. 5. Absorption cross sections from Ref. 1, plotted with the same conventions used in Fig. 2. Here the calculations use parameter set E , with π^+ given by the solid line and π^- by the dashed line.

the reactive parameters of parameter set F at 50 MeV are also given, in brackets, in Table IV, for comparison. For pionic atoms set E is the same as parameter set A of Ref. 3. For other energies the parameters were inferred by linear interpolation, except for the quasielastic reactive parts $\text{Im}b$, $\text{Im}c$ which were calculated. The resultant calculated absorption cross sections are plotted, compared to the experimental results of Ref. 1, in Fig. 5, and the calculated elastic scattering is compared with experiment for 30, 40, and 50 MeV π^+ scattering in Fig. 6. It should be noted that we only show the data from Refs. 6 and 7, although data from other targets⁸ was included in the fit. Discrepancies among the data are the principle reason for the disagreements between calculation and experi-

ment for ^{12}C at 50 MeV.

These figures demonstrate that a reasonable compromise fit to absorption and elastic scattering results has been obtained with this set of parameters in the low energy region. Figure 5 indicates that there still might be an isovector effect in absorption, particularly in the low energy region, but the systematic errors, and the lack of π^- elastic scattering data, make it difficult to assess it quantitatively. The parameters of Table IV indicate that the absorptive parameters decrease with energy in this range, while the quasielastic reactive part increases.

VII. DISCUSSION

The values of the absorption parameters discussed here depend on the other parameters of the potential, in particular on the LLEE parameter λ . We have shown that the arguments are independent of λ over the range $\lambda \sim 1-2$. The question arises whether the results can be cast in a more invariant form. The extent to which complicated potentials of the form (1) can be replaced by a simple 4-parameter equivalent Kisslinger potential

$$2\omega U = -4\pi b_{\text{eff}}\rho(r) + 4\pi c_{\text{eff}}\vec{\nabla}\rho(r)\cdot\vec{\nabla} - 4\pi c_{\text{eff}}\frac{\omega}{2m}\nabla^2\rho(r) \quad (4)$$

has been discussed by many authors, particularly by Seki¹¹ and collaborators. For pionic atoms, this can be done over a wide region of parameter space, making it possible to reduce many analyses to a common form. We reduced the optical potential to the form (4) following the prescription of Ref. 3. This is not particularly accurate, so we repeated the π -atom analysis and the 50 MeV π^+ elastic scattering analysis with a potential of the form (4). In the π^+ scattering analysis the fit was constrained by demanding only small variations in the s and p wave parameters separately from their pionic atom values. The result is the parameter set K_1 shown in Table V for π^- atoms and for 50 MeV π^+ elastic scattering. The reaction cross section at 50 MeV predicted by this fit is given in Table II. The values in Table V show that the reactive parameters of the optical potential are approximately constant with energy in region 0–50 MeV. Comparing with parameter set E in Table IV, this indicates that the decrease in absorption parameters is compensated by the increase in the

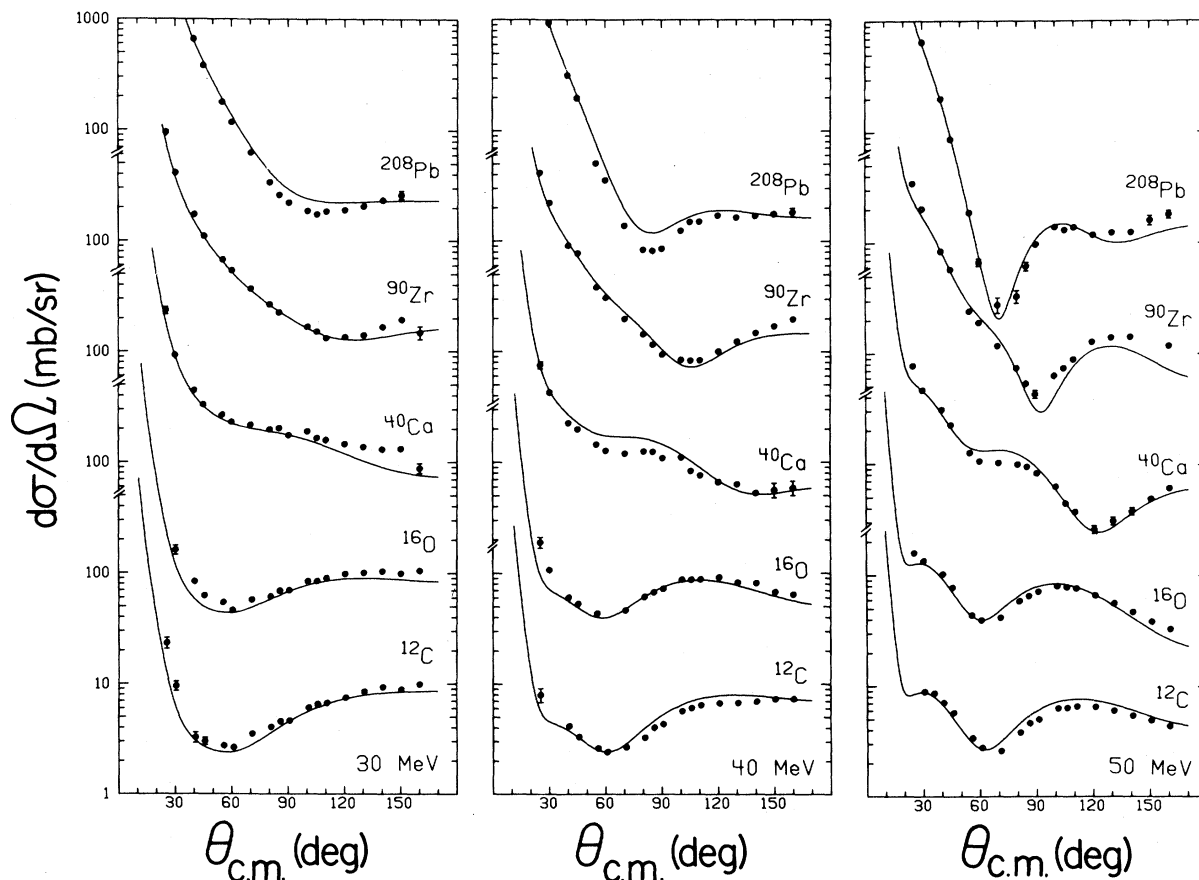


FIG. 6. Elastic π^+ scattering data from Refs. 6 and 7 compared to the calculations using parameter set E . The potential parameter set used here is the same as the one used in Fig. 5, providing a systematic analysis consistent with the scattering and pionic atom data.

quasielastic reactive part. Significant changes in the total reactive content of the optical potential with energy in this range come not from the variation of the parameters but from the p -wave $\nabla \cdot \rho \nabla$ term which behaves like k^2 , increasing by a factor ~ 3 in going from 20 to 50 MeV.

Much better fits to elastic scattering have been

obtained by other groups by free variation of parameters as a function of energy and nucleus, without using the constraints imposed by pionic atom data. A recent example is an analysis by Amann *et al.*,¹⁰ mostly on ^{12}C data, using a 4-parameter potential of the form (4) but without the last term coming from kinematics (angle transfer-

TABLE IV. Parameter set E , used in the calculations shown in Figs. 5 and 6, at 0, 25, and 50 MeV. For comparison, the reactive parameters for set F at 50 MeV are given in brackets.

	π -atom	25 MeV	50 MeV	
b_0 (fm)	-0.046	$-0.053 + 0.002i$	$-0.061 + 0.006i$	(0.004i)
b_1 (fm)	-0.13	$-0.13 - 0.001i$	$-0.13 - 0.002i$	(-0.001i)
c_0 (fm ³)	0.66	$0.68 + 0.007i$	$0.70 + 0.028i$	(0.017i)
c_1 (fm ³)	0.43	$0.44 + 0.004i$	$0.46 + 0.013i$	(0.008i)
λ	1.4	1.4	1.4	
B_0 (fm ⁴)	$0.007 + 0.19i$	$-0.006 + 0.16i$	$-0.02 + 0.11i$	(0.16i)
C_0 (fm ⁶)	$0.29 + 0.93i$	$0.32 + 0.74i$	$0.36 + 0.54i$	(0.77i)

TABLE V. Four parameter potential sets corresponding to Eq. (4). K_1 is given at zero (π atom) and 50 MeV, and obeys the constraints that all parameters vary slowly between 0 and 50 MeV. K_2 is an unconstrained fit for π^+ at 50 MeV.

	K_1 (π atom)	K_1 (50 MeV)	K_2 (50 MeV)
b_0 (fm)	$-0.045 + 0.015i$	$-0.068 + 0.017i$	$-0.069 + 0.006i$
c_0 (fm ³)	$0.51 + 0.034i$	$0.55 + 0.038i$	$0.56 + 0.091i$

mation). Their fit put most of the reactive strength into the p -wave term, $\text{Im}c_{\text{eff}}$, which remained approximately constant in the energy range 30–60 MeV, while the s -wave parameter $\text{Im}b_{\text{eff}}$ decreased with energy, and in fact became negative. We found a similar effect in an unconstrained four parameter analysis using the full equation (4), obtaining set K_2 at 50 MeV, which has a large value for $\text{Im}c_{\text{eff}}$ and a very small, but positive, value for $\text{Im}b_{\text{eff}}$. Yoo and Landau¹² have shown that this difference between a small but positive and a negative $\text{Im}b_{\text{eff}}$ can be understood, at least qualitatively, as a purely kinematical effect. Another way of including the angle transformation, instead of the third term in equation (3), is the replacement

$$b_{\text{eff}} \rightarrow b_{\text{eff}} - \frac{\omega}{2m} k^2 c_{\text{eff}},$$

which causes $\text{Im}b_{\text{eff}}$ to decrease with energy and eventually change sign. Thus the negative value of $\text{Im}b_0$ found by Amman *et al.*¹⁰ is a result of implicitly including this kinematic term in their s -wave parameters.

Note that for parameter set K_2 , which is not constrained by smooth variation from pionic atom parameters, a sizable increase in σ_R is obtained for light but not for heavy nuclei. It is therefore possible that, in the general fit, if we allowed the s -wave absorption parameter to decrease markedly, and the p -wave absorption parameter to increase with energy, it would be possible to accommodate both larger quasielastic and absorption cross sections to the elastic scattering for light and medium weight nuclei. The reason we did not do so is that in fitting π^- deuteron absorption, no such effect is observed.⁵ On the other hand, the absorption parameters of Ref. 5 do not agree either in absolute magnitude or energy variation with any of the fitted sets.

VIII. CONCLUSION

We have fit most low energy pion data with an optical potential that has four parameters fitted at zero energy, smoothly connected to three parameters fitted at 50 MeV, with all other parameters taken from theoretical calculations. The π^+ elastic scattering data are fitted rather well with different data sets tending to bracket the calculations. The energy dependence of the absorption data is well described with the resulting parameters, but there is a systematic normalization difference. The few data on quasielastic scattering, from light nuclei, are consistent with the fit.

In fitting elastic scattering we have always averaged over elements and over different data sets. This global approach averages over any deficiencies of the optical model as well as the normalization and other systematic uncertainties in the data. The parameter values determined do, however, reflect certain biases used to overcome the incompleteness of existing data. Specifically we chose the pionic atom (π^-) and 50 MeV π^+ elastic scattering as the fiducial points for defining the reaction cross section, since these appear to be the best determined data at present. This reaction cross section was used as the basis for deciding the division between quasielastic and absorption cross sections. However, the reaction cross section is not determined uniquely this way. As Table II shows, the reaction cross section, as a function of A , is sensitive to the form of the potential, in particular to the division of the absorption parameters between s and p wave parts. Also, Coulomb effects are very important in this energy region, and are amplified by the velocity-dependent p -wave term of the optical potential. The difference between π^+ and π^- scattering could be quite sensitive to changes in the potential, such as adding the gauge terms proposed by Ericson.¹³ It would be more logical to connect

π^- scattering smoothly to pionic atom parameters. It is very important to measure the reaction cross sections as well as π^- elastic scattering to reduce these ambiguities. We used the argument that the measured cross section for π^+ absorption was uncomfortably close to the σ_R inferred from elastic scattering to justify a 20% normalization of the measured absorption. Independent measurements of σ_R and σ_{qe} would determine whether this is acceptable or not, particularly for heavy elements, where σ_R seems less dependent on the form of the potential. Because of the compromises that had to be made, it was impossible to say anything about the isovector component of absorption. Absorption measurements on a series of isotopes could eliminate systematic errors in both experiment and analysis, and give a better prospect of identifying this component. The present analysis indicates that the absorptive parameters show a slow decrease with energy in this energy range 0–50 MeV, instead of the mild increase expected on the basis of simple microscopic calculations. This threshold behavior must change at some point, as a resonant behavior is expected for these parameters, so that continuing this analysis to higher energies would be of considerable interest. However, if the parameters in the optical potential are to be compared with microscopic predictions, it is not possible to calculate absorption cross sections from formula (2) except at low energies. In general it is

necessary to use the optical model parameters as the input to a transport calculation in order to determine partial cross sections. This has been dealt with in an optical model context by Masutani and Yazaki.¹⁴ Thus at higher energies the reaction cross section σ_R is the only one which can be directly compared with the predictions of the optical potential.

In conclusion, we have shown how a global analysis can fit existing data and point towards important areas for further study. The particular compromise fit adopted here is not strongly preferred, but indicates the general behavior of the parameters. It remains to be seen whether the behavior of the absorption parameters can be explained in a microscopic model, and what information can be gleaned from π^- and σ_R measurements.

ACKNOWLEDGMENTS

We wish to thank R. A. Eisenstein and R. Seki for providing us with the codes PIRK¹⁵ and MATOM,¹⁶ modified versions of which were used in the calculations, and B. M. Freedom for providing us with some data far in advance of publication. This work was supported by the National Science Foundation under Grant No. PHY-7922054.

*Present address: Physics Department, The Florida State University, Tallahassee, Florida 32306.

¹K. Nakai *et al.*, Phys. Rev. Lett. **44**, 1446 (1980).

²K. Stricker, H. McManus, and J. A. Carr, Phys. Rev. C **19**, 929 (1979).

³K. Stricker, J. A. Carr, and H. McManus, Phys. Rev. C **22**, 2043 (1980).

⁴G. E. Brown, B. K. Jennings, and V. Rostokin, Phys. Rep. **50C**, 227 (1979).

⁵J. Chai and D. O. Riska, Nucl. Phys. **A329**, 429 (1979).

⁶B. M. Freedom *et al.*, Phys. Rev. C **23**, 1134 (1981).

⁷M. Blecher *et al.*, Phys. Rev. C **20**, 1884 (1979).

⁸S. A. Dytman *et al.*, Phys. Rev. C **19**, 971 (1979).

⁹T. J. Bowles *et al.*, Phys. Rev. C **23**, 439 (1981).

¹⁰J. F. Amman *et al.*, Phys. Rev. C **23**, 1635 (1981).

¹¹R. Seki, K. Masutani, M. Oka, and K. Yazaki, Phys. Lett. **97B**, 200 (1980).

¹²K. B. Yoo and R. H. Landau, Oregon State Report (unpublished).

¹³T. E. O. Ericson, Abstracts of Contributed papers, Ninth International Conference on High Energy Physics and Nuclear Structure, Versailles, 1981 (unpublished), paper G 10, 258, 1981; T. E. O. Ericson and L. Tauscher, *ibid.*, paper I 9, 354, 1981.

¹⁴K. Masutani and K. Yazaki, see Ref. 13, paper G 31, 279, 1981; Phys. Lett. (to be published).

¹⁵R. A. Eisenstein and G. A. Miller, Comput. Phys. Commun. **8**, 130 (1974).

¹⁶R. Seki, private communication.